Scaling of Divertor Heat Flux Profile Widths in DIII-D*

C.J. Lasnier, M.A. Makowski, J.A. Boedo, N.H. Brooks,
A.W. Leonard, J.G Watkins, and W.P. West

Background

The width of the divertor heat flux profile $w_{q,div}$ is of great interest in future large tokamaks as well as many present devices. Previous studies examining the parametric dependence of $w_{q,div}$ have arrived at diverse scalings [1] in JET [2], ASDEX-Upgrade [3], JT60-U [4,5], DIII-D [6,7], and NSTX [8] with results somewhat at variance with each other. We attempt here to perform a new series of experiments in DIII-D to obtain scaling of the divertor heat flux peak value, profile width, and divertor plate power as a function of plasma input parameters, with the maximum number of divertor and scrape-off-layer (SOL) diagnostics brought to bear. This data will be incorporated in an effort to improve understanding of SOL transport

[1] A. Loarte, *et al.*, Nucl Fusion **47**, S203 (2007).
[2] T. Eich, *et al.*, J. Nucl. Mater. **337–339**, 669 (2005).
[3] A. Herrmann, Plasma Phys. Control. Fusion **44**, 883 (2002).
[4] ITER Physics Basis Editors, Nucl. Fusion **39**, 2137 (1999).
[5] A. Loarte, *et al.*, J. Nucl. Mater. **266–269**, 587 (1999).
[6] D.N. Hill, *et al.*, J. Nucl. Mater. **196–198**, 204 (1992).
[7] C.J. Lasnier, *et al.*, Nucl. Fusion **38**, 1225 (1998).
[8] R. Maingi, *et al.*, J. Nucl. Mater. **363–365**, 196 (2007).

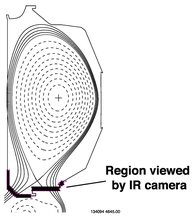

Experimental procedure

We performed measurements in lower single-null edge localized mode (ELM) H-mode diverted configurations that, due to the strike-point positions, were not strongly pumped. We varied the plasma current I_p at constant toroidal field B_T, and varied line-averaged density $\bar{n}_e$ at constant I_p and B_T. The neutral beam injected power P_{inj} was changed at constant I_p and B_T, B_T at constant I_p, and B_T at constant q_{95}. The divertor heat flux was calculated from infrared camera measurements using a new high-resolution fast-framing IR camera.

Representative time trace

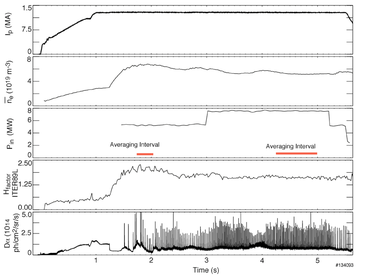

Analysis method

For each discharge, one or more time intervals of interest were selected where plasma conditions varied little during the interval. The average of each quantity was compiled for each interval. Low-frequency ELMs are included in the average with only small effect.

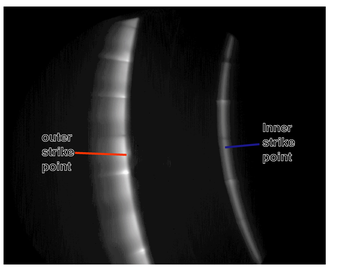

Typical DIII-D divertor IR camea image with pre-shot image subtracted. The divertor is viewed from above. #134078_9747

IR camera and heat flux analysis

The IR camera recorded divertor plate surface thermal emission at multi-kilohertz frame rates through the whole discharge to allow measuring rapid changes due to ELMs, which we time-averaged as needed. The heat flux at each position in the radial profile was calculated at each of the times steps using the THEODOR 2D heat flux analysis code [9].

The code accounts for 2D heat transport in the divertor tiles, which is needed for pulse length -> 4 s. We show scaling of the divertor peak heat flux and profile width as a function of the parameters varied, and compare with published results from other devices.

[9] A. Herrmann et al., Plasma Phys. Control. Fusion **37,** 17 (1995)

*Work supported by the US Department of Energy under DE -A C52 -07NA 27344, DE - FG02 -07ER54917, DE -FC02 -04ER54698, and DE -A C04 -94A L85000 .

Presented at EPS 2009 Sofia, Bulgaria

Peak Divertor Heat Flux q_{peak}

Inner and outer strike point peak heat fluxes vary linearly with input power

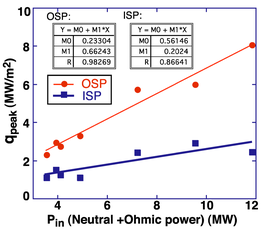

Fig. 1

Power scan:

I_p = 1.3 MA, B_T = -1.9 T were held constant. Density was between 5.2 and 6.5x10^{19} m^{-3}, except at the highest power, where $\bar{n}_e$ = 2.3x10^{19} m^{-3}.

Divertor Heat Flux Profile Width $\lambda_{q,FWHM}$

Weak dependence of width on input power

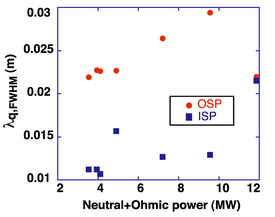

Comparison with previous results

This scaling: $q_{peak} \propto$ Power in

$\lambda_{q,FWHM}$ depends weakly on Power in

Peak heat flux: Linear scaling with power agrees with ASDEX-Upgrade DIV-II, NSTX, DIII-D previous scaling, JET (IR) ASDEX-Upgrade DIV-I found $q_{peak} \propto P^{0.5+/-0.05}_{target}$.

Heat flux width:

Other studies found $q_{peak} \propto P^{-.01}$ to $P^{+0.4}$

Previous DIII-D scaling also had q_{peak} P_{in}

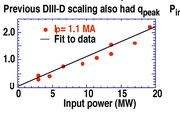

Peak heat flux drops linearly as density increases

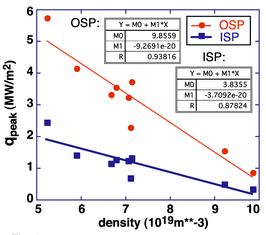

Fig. 2

Density scan:

P_{inj} = 4.6-4.7 MW except for the densities 5.2x10^{19} m^{-3}, where P_{inj} = 7 MW, and 6.8x10^{19} m-3 where P_{inj} = 3.8 MW. Toroidal field was held constant at B_T = -1.9 T, and plasma current was held at I_p = 1.3 MA.

Heat flux peaks become lower and broader at high density (detachment)

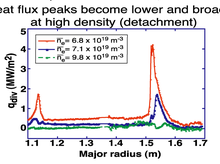

The heat flux profile broadens at onset of detachment

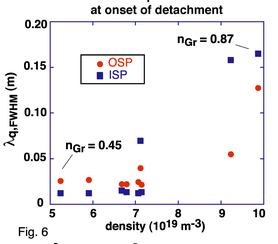

Fig. 6

This scaling: $q_{peak} \propto -\bar{n}_e$

$\lambda_{q,FWHM}$ broadens at onset of detachment

From ASDEX-U DIV-I [3], $q_{peak} \propto n_e^{-0.77}$

and ASDEX-U DIV-II : $q_{peak} \propto n_e^{-1.0}$

Peak heat flux increases linearly with plasma current

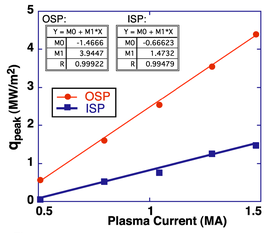

Fig. 3

Plasma current scan:

B_T = -1.9 T, and P_{inj} = 4.65-4.8 MW except for the point at I_p = 1.3 MA where P_{inj} = 3.8 MW. Natural H-mode density (no puffing)

Density variation during Ip scan was within the range where profile width is unaffected (See Fig. 6)

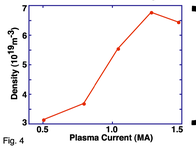

Fig. 4

Heat flux profile width varies inversely with plasma current.

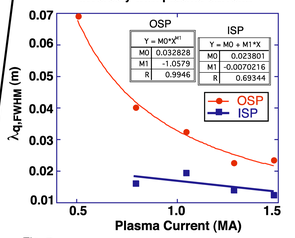

Fig, 7

This scaling: $q_{peak} \propto I_p$ (natural H-mode density)

$\lambda_{q,FWHM} \propto 1/I_p$

These are both consistent with NSTX [8]. Previous DIII-D scaling[7] also found peak heat flux scaled like I_p.

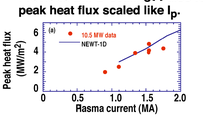

Divertor heat flux profile width dropped linearly as Bt increased at nearly constant safety factor

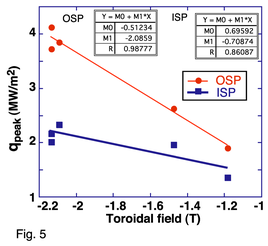

Fig. 5

B_T scan at constant q_{95}

q_{95} = 3.6-3.7

Density range was $\bar{n}_e$ = 3.2x10^{19} m^{-3} at the lowest field to $\bar{n}_e$ = 5.8x10^{19} m^{-3} at the highest field.

Profile width varies linearly with B_T at nearly constant safety factor

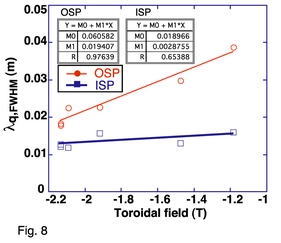

Fig. 8

This scaling: $q_{peak} \propto |B_T|$

$\lambda_{q,FWHM} \propto -B_T$

Previous DIII-D scaling found peak heat flux scaled like $1/B^{0.5}$ for constant I_p, which was close to linear over the data range. This was not at constant q_{95}.